Journal of Ethnopharmacology 259 (2020) 112945

Contents lists available at ScienceDirect

Journal of Ethnopharmacology

journal homepage: www.elsevier.com/locate/jethpharm

Antiviral activity of furanocoumarins isolated from *Angelica dahurica* against influenza a viruses H1N1 and H9N2

Ba Wool Lee[a], Thi Kim Quy Ha[a,b], Hyo Moon Cho[a], Jin-Pyo An[a], Seong Kyun Kim[c], Choong-Sik Kim[c], Eunhee Kim[c], Won Keun Oh[a,*]

[a] Korea Bioactive Natural Material Bank, Research Institute of Pharmaceutical Sciences, College of Pharmacy, Seoul National University, Seoul, 08826, Republic of Korea
[b] College of Natural Sciences, Cantho University, Campus II, Cantho City, Viet Nam
[c] Choong Ang Vaccine Laboratory, 1476-37, Yuseong-daero, Yuseong-gu, Daejeon, 34055, Republic of Korea

ARTICLE INFO

Keywords:
Angelica dahurica
Furanocoumarin
Influenza
Neuraminidase
H1N1
Polymerase acidic protein

ABSTRACT

Ethnopharmacological relevance: *Angelica dahurica* (Hoffm.) Benth. & Hook.f. ex Franch. & Sav. (Umbelliferae family) is an herbaceous, perennial plant native to northern and eastern Asia. The root of *A. dahurica* has traditionally been used under the name "Bai Zhi" as a medicinal plant for colds, dizziness, ulcers, and rheumatism. Moreover, it is also an important ingredient of various prescriptions, such as Gumiganghwal-Tang, for the common cold and influenza.

Aim of the study: Even though various biological activities of the root of *A. dahurica* have been reported along with its chemical components, the detailed mechanism of how it exerts anti-influenza activity at the compound level has not been studied. Therefore, we investigated the anti-influenza properties of furanocoumarins purified by bioactivity-guided isolation.

Materials and methods: Bioactivity-guided isolation from a 70% EtOH extract of the root of *A. dahurica* was performed to produce four active furanocoumarins. The inhibition of cytopathic effects (CPEs) was evaluated to ascertain the antiviral activity of these compounds against influenza A (H1N1 and H9N2) viruses. The most potent compound was subjected to detailed mechanistic studies such as the inhibition of viral protein synthesis, CPE inhibition in different phases of the viral replication cycle, neuraminidase (NA) inhibition, antiapoptotic activity using flow cytometry, and immunofluorescence.

Results: The bioactivity-guided isolation produced four active furanocoumarins, isoimperatorin (**1**), oxypeucedanin (**2**), oxypeucedanin hydrate (**3**) and imperatorin (**4**) from the *n*-BuOH fraction. Among them, compound **2** (followed by compounds **1**, **4** and **3**) showed a significant CPE inhibition effect, which was stronger than that of the positive control ribavirin, against both H1N1 and H9N2 with an EC_{50} (μM) of 5.98 ± 0.71 and 4.52 ± 0.39, respectively. Compound **2** inhibited the synthesis of NA and nucleoprotein (NP) in a dose-dependent manner. In the time course assays, the cytopathic effects of influenza A-infected MDCK cells were reduced by 80–90% when treated with compound **2** for 1 and 2 h after infection and declined drastically 3 h after infection. The level of viral NA and NP production was markedly reduced to less than 20% for both proteins in compound **2** (20 μM)-treated cells compared to untreated cells at 2 h after infection. In the molecular docking analysis, compound **2** showed a stronger binding affinity for the C-terminus of polymerase acidic protein (PAC; −36.28 kcal/mol) than the other two polymerase subunits. Compound **2** also exerted an antiapoptotic effect on virus infected cells and significantly inhibited the mRNA expression of caspase-3 and Bax.

Conclusion: Our results suggest that compound **2** might exert anti-influenza A activity via the inhibition of the early phase of the viral replication cycle, not direct neutralization of surface proteins, such as hemagglutinin and NA, and abnormal apoptosis induced by virus infection. Taken together, these findings suggest that furanocoumarins predominant in *A. dahurica* play a pivotal role in its antiviral activity. These findings can also explain the reasons for the ethnopharmacological uses of this plant as an important ingredient in many antiviral prescriptions in traditional Chinese medicine (TCM).

* Corresponding author.
E-mail address: wkoh1@snu.ac.kr (W.K. Oh).

https://doi.org/10.1016/j.jep.2020.112945
Received 24 January 2020; Received in revised form 16 April 2020; Accepted 1 May 2020
Available online 07 May 2020
0378-8741/

1. Introduction

The world health organization (WHO) stated that approximately three quarters of world's population depends on natural medicine, mainly medicinal plants in different civilizations (Gilani and Rahman, 2005). Many countries have utilized a variety of formulas composed of various medicinal plants for the treatment of viral infection, such as influenza. Though pure compounds and synthetic drugs, which represent conventional medicine today, largely replaced the use of herbal medicine, there is a growing recognition of the herbal medicine as its effectiveness have been investigated scientifically (Eng et al., 2019). Anti-influenza properties of some representative formulas in traditional Korean medicine, such as Ma-Huang-Tang, and Galgeun-Tang were previously reported. Ma-Huang-Tang, which is composed of four medicinal plants and commonly used for treating the acute upper respiratory infection, was shown to reduce cytopathic effect induced by H1N1 infection and significantly attenuate histopathological changes and excessive secretion of inflammatory cytokines in an ICR pneumonia mouse model (Wei et al., 2018). Also, Galgeun-Tang, which is used for the patients with symptoms of headache, stiffness of neck, and fever, was reported to exert anti-influenza activity by increasing IL-12 production in the early phase of viral cycle (Kurokawa et al., 2002). A clinical trial demonstrated that a time to fever resolution in H1N1-infected participants was reduced by 19% in the group of patients prescribed with a combination of oseltamivir and maxingshigan-yinqiaosan compared to the group with oseltamivir C. Wang et al., 2011). Gumiganghwal-Tang (jiuweiqianghuo tang) listed in Dong-Eu-Bo-Gam (Heo, Joon, AD 1713) of Korea ancient pharmacopoeias, has been used for common cold and influenza with headache, body aches and fever regardless of seasons (Moon et al., 1999; Jin et al., 2014). As main one of its constituting medicinal herb, *Angelica dahurica* (under the name “Bai Zhi” in China) contributes to its overall activity by exerting antipyretic, analgesic, and anti-inflammatory properties (Choi et al., 2008).

Angelica dahurica (Hoffm.) Benth. & Hook.f. ex Franch. & Sav., a perennial plant of the Umbelliferae (*alt.* Apiaceae), is widely distributed in northeastern China and Korea. The root of *A. dahurica* is used as a traditional folk medicine in China and Korea for abscesses, headaches, the common cold, fever, inflammation, flu, etc (Sarker and Nahar, 2004). Various laboratory-identified biological activities have been reported, including anti-inflammatory (Kang et al., 2007), anti-influenza A (Park and Lee, 2005), antiobesity (Lu et al., 2016), wound healing (Zhang et al., 2017) and antioxidant (Pervin et al., 2014) activities at even crude extract levels. For more detail, active compounds with a myriad of activities, such as anticancer (Luo et al., 2011), antibacterial, antifungal (Walasek et al., 2015), antiallergy (Xian et al., 2019), antihypertension (Zhang et al., 2011), cholinesterase inhibition (Tun and Kang, 2017), anti-human immunodeficiency virus (HIV), and anti-herpes simplex virus (HSV) activity (Koziol and Skalicka-Woźniak, 2016), have been studies. In addition, *A. dahurica* contains coumarin as the major class of compounds in the *Angelica* genus (Shokoohinia, 2014), steroids (Li and Wu, 2017), and aromatic essential oil attributed to myriad of monoterpenes and sesquiterpenes (Kim and Chi, 1990). Although there have been many studies about the bioactivity of the constituents isolated from *A. dahurica* in terms of their traditional uses, such as sweat-inducing herbs to combat harmful external pathogens, few studies about the direct antiviral property of compounds against influenza A virus have been conducted. Therefore, based on our screening data combined with literature reviews, we performed bioactivity-guided isolation and examined the efficacies of the isolates along with performing detailed mechanistic studies of the most active compound by using CPE assays, Western blotting, immunofluorescence, flow cytometry, etc. Moreover, we determined the content of these isolated compounds in the 70% EtOH total extract to determine the activity of the extract and the history of ethnopharmacological uses.

2. Materials and methods

2.1. General information

A JEOL 600 MHz spectrometer (JEOL, Tokyo, Japan) with deuterated solvents was used for nuclear magnetic resonance (NMR) spectroscopy. Column chromatography (CC) was performed using various resins, including silica gel (particle size: 63–200 μm, Zeochem AG, Rüti, Switzerland) and reversed-phase (RP) C_{18} (particle size: 40–63 μm, Nacalai Tesque, Kyoto, Japan). Silica gel 60 F_{254} and RP-18 $F_{254}S$ thin-layer chromatography (TLC) plates were purchased from Merck (Darmstadt, Germany). A Gilson high-performance liquid chromatography (HPLC) system was utilized at a flow rate of 2 mL/min with UV detection at 205 and 254 nm using an Optima Pak C18 column (10 × 250 mm, 10 μm particle size; RS Tech, Seoul, Korea). Industrial-grade MeOH and EtOH and *n*-BuOH were used for extraction and fractionation. Analytical-grade MeOH and MeCN were used for isolation and analysis. All solvents were purchased from Daejung Chemical (Siheung, Korea).

2.2. Plant material

The roots of *Angelica dahurica* were purchased from Duk-hyun dang, herbal medicine market, located in Seoul (Republic of Korea). A voucher specimen (SNU2016-06) of *A. dahurica* was stored at the Korea Bioactive Natural Material Bank, Research Institute of Pharmaceutical Science, College of Pharmacy, Seoul National University, Seoul, Republic of Korea.

2.3. Extraction and isolation of furanocoumarins from A. dahurica

The roots of *A. dahurica* (0.6 kg) were extracted with 70% EtOH (3 times, 4 L each) at room temperature. The crude extract was dried *in vacuo* by an evaporator to obtain 70% EtOH extract (55 g), which was suspended in water and fractionated with *n*-BuOH. The *n*-BuOH soluble extract (35 g) was subjected to silica gel CC (20 × 60 cm) with a gradient solvent system of *n*-hexane/acetone (20/1 → 2/1 [v:v]) to obtain 5 subfractions (F1–F5). Subfraction F1 (2.0 g) was subjected to reverse-phase CC (5 × 60 cm) with an isocratic system of MeOH/H_2O (75/25) to obtain F1.2 (260 mg) from which isoimperatorin (**1**, 27.5 mg) (Bergendorff et al., 1997) was isolated through recrystallization. Subfraction F2 (2.6 g) was subjected to reverse-phase CC (5 × 60 cm) with an isocratic system of MeOH/H_2O (75/25) to obtain 5 subfractions (F2.1 − F2.5). F2.1 was rechromatographed under the same conditions to obtain F2.1.1 and F2.1.2. F2.1.2 (50 mg) was subjected to reverse-phase semi-preparative HPLC with a gradient system of MeOH/H_2O (0–15 min, 65/35, 15–25 min, 76/24), resulting in the isolation of imperatorin (**4**, 9.7 mg) (Harkar et al., 1984). Subfraction F3 (2.2 g) was subjected to reverse-phase CC (5 × 60 cm) with an isocratic system of MeOH/H_2O (75/25) to obtain 5 subfractions (F3.1 − F3.5). F3.2 (580 mg) was rechromatographed under the same conditions to obtain F3.2.1 − F3.2.12. F3.2.3 (50 mg) was subjected to reverse-phase semi-preparative HPLC with an isocratic system of MeCN/H_2O (40/60), resulting in the isolation of oxypeucedanin hydrate (**3**, 1.2 mg) (Tavakoli et al., 2018). From this fraction, oxypeucedanin (**2**, 24.2 mg) (Bergendorff et al., 1997) was also obtained by crystallization.

2.4. Physical and spectroscopic information of the compounds

Isoimperatorin (**1**): white solid; ESI-MS *m/z*: 271 $[M + H]^+$; ^{1}H-NMR (300 MHz, $CDCl_3$): δ_H 6.22 (1H, d, J = 9.6 Hz, H-3), 8.11 (1H, d, J = 9.6 Hz, H-4), 7.10 (1H, s, H-8), 7.56 (1H, d, J = 2.4 Hz, H-2′), 6.92 (1H, d, J = 2.4 Hz, H-3′), 4.88 (2H, d, J = 7.2 Hz, H-1″), 5.50 (1H, m, H-2″), 1.77 (3H, s, H-4″), 1.67 (3H, s, H-5″); ^{13}C-NMR (75 MHz, $CDCl_3$): δ_C 161.2 (C-2), 112.5 (C-3), 139.5 (C-4), 148.9 (C-5), 114.2 (C-6), 158.1

(C-7), 94.1 (C-8), 152.6 (C-9), 107.5 (C-10), 144.8 (C-2′), 105.0 (C-3′), 69.7 (C-1″), 119.1 (C-2″), 139.7 (C-3″), 25.7 (C-4″), 18.2 (C-5″).

Oxypeucedanin (**2**): white solid; ESI-MS *m/z*: 287 $[M + H]^+$; ^{1}H-NMR (300 MHz, $CDCl_3$): δ_H 6.26 (1H, d, J = 9.9 Hz, H-3), 8.16 (1H, d, J = 9.9 Hz, H-4), 7.58 (1H, d, J = 2.1 Hz, H-2′), 6.91 (1H, d, J = 2.1 Hz, H-3′), 4.58 (1H, dd, J = 4.2, 10.8 Hz, H-1″a), 4.39 (1H, dd, J = 6.6, 10.8 Hz, H-1″b), 3.20 (1H, dd, J = 4.2, 6.6 Hz, H-2″), 1.38 (3H, s, H-4″), 1.30 (3H, s, H-5″); ^{13}C-NMR (75 MHz, $CDCl_3$): δ_C 160.9 (C-2), 113.0 (C-3), 138.9 (C-4), 148.3 (C-5), 114.1 (C-6), 157.9 (C-7), 94.7 (C-8), 152.4 (C-9), 107.3 (C-10), 145.2 (C-2′), 104.4 (C-3′), 72.2 (C-1″), 61.1 (C-2″), 58.3 (C-3″), 24.6 (C-4″), 19.0 (C-5″).

Oxypeucedanin hydrate (**3**): yellow amorphous powder; ESI-MS *m/z*: 305 $[M + H]^+$; ^{1}H-NMR (300 MHz, $CDCl_3$): δ_H 6.13 (1H, d, J = 9.0 Hz, H-3), 8.13 (1H, d, J = 9.0 Hz, H-4), 7.56 (1H, d, J = 2.4 Hz, H-2′), 6.90 (1H, d, J = 2.4 Hz, H-3′), 5.36 (1H, m, H-2″), 4.60 (2H, m, H-1″), 1.33 (6H, s, H-4″ and H-5″); ^{13}C-NMR (75 MHz, $CDCl_3$): δ_C 160.8 (C-2), 111.9 (C-3), 139.7 (C-4), 148.9 (C-5), 113.5 (C-6), 157.7 (C-7), 93.5 (C-8), 145.1 (C-9), 106.7 (C-10), 144.6 (C-2′), 105.0 (C-3′), 74.7 (C-1″), 76.5 (C-2″), 71.1 (C-3″), 25.1 (C-4″ and 5″).

Imperatorin (**4**): white solid; ESI-MS *m/z*: 271 $[M + H]^+$; ^{1}H-NMR (300 MHz, $CDCl_3$): δ_H 6.34 (1H, d, J = 9.6 Hz, H-3), 7.74 (1H, d, J = 9.6 Hz, H-4), 7.33 (1H, s, H-5), 7.66 (1H, d, J = 2.4 Hz, H-2′), 6.79 (1H, d, J = 2.4 Hz, H-3′), 4.98 (2H, d, J = 6.9 Hz, H-1″), 5.59 (1H, m, H-2″), 1.71 (3H, s, H-4″), 1.69 (3H, s, H-5″); ^{13}C-NMR (75 MHz, $CDCl_3$): δ_C 160.5 (C-2), 114.6 (C-3), 143.7 (C-4), 113.1 (C-5), 125.8 (C-6), 148.5 (C-7), 131.6 (C-8), 143.7 (C-9), 116.4 (C-10), 146.6 (C-2′), 106.7 (C-3′), 70.1 (C-1″), 119.7 (C-2″), 139.7 (C-3″), 25.8 (C-4″), 18.1 (C-5″).

2.5. Quantitative analysis of four active furanocoumarins by high-pressure liquid chromatography with diode array detection (HPLC-DAD)

To analyze the contents of the four compounds, 10 mg/mL standard stock solutions of compounds **1**–**4** with purities greater than 99.0, 96.3, 99.0 and 99.0% (by HPLC) were prepared with methanol or acetone (Figs. S2–S5). They were stored sealed in a fridge and diluted to make working solutions with appropriate concentrations. Quantitative analysis was carried out using a Thermo Fisher UltiMate 3000 HPLC system (Germering, Germany) with DAD. The separation was achieved using a Phenomenex Kinetex C_{18} column (250 × 4.6 mm, 5.0 μm, 100 Å; Torrance, CA, USA) maintained at 30 °C. A step gradient system using an aqueous acetonitrile (MeCN) system (A: H_2O/B: MeCN containing 0.1% formic acid) over 35 min (0.0–6.0 min, 33% B/6.1–18.0 min, 41% B/18.1–25.0 min, 65% B) at a flow rate of 1 mL/min. Ten microliters of solution was injected for every analysis, and a 310 nm wavelength was applied. Under these optimal conditions, four compounds were well separated from each other and quantified accurately (Fig. S1). A 10 mg/mL 70% EtOH extract of *A. dahurica* was prepared in 100% MeOH for quantitative analysis.

2.6. Calibration curve, linearity, LOD and LOQ

After the HPLC analysis of 70% EtOH extract was performed to obtain approximate peak areas of each compound, working solutions of standard compounds at five different concentrations (Table 1) were made, and their linearities were established by plotting the peak area (y) vs. the quantity per injection (x) of a compound, which was expressed by the regression equation. Regression parameters of the slope, intercept and correlation factor (R) were calculated based on the linear regression data analysis tool in Microsoft Excel. The limit of detection (LOD) and limit of quantification (LOQ) were defined as concentrations corresponding to a signal-to-noise (S/N) ratio of 3 and 10, respectively. From the linearity data, the LOD and LOQ were calculated by $3\sigma/S$ and $10\sigma/S$, where σ represents the standard deviation of the values and S represents the slope of the calibration curve. Analytical method for the linearity, LOD and LOQ was validated according to the International Conference on Harmonization guidelines (ICH, 1996) and relevant papers on quantitative analysis (An et al., 2019; Liu et al., 2013).

2.7. Precision and accuracy

The precision was analyzed at three different concentrations (low, middle and high) covering the concentrations of each test compound. Working solutions were prepared in triplicate at each concentration to validate the method precision. Three samples of each standard compound were analyzed on the same day to determine the intraday precision. Three samples were also analyzed on three consecutive days to determine the interday precision. For the accuracy test, three standard working solutions with concentrations of approximately 50%, 100% and 150% compared to the content of analytes in the extract were spiked into the 70% total extract of 10 mg/mL at a 1:1 ratio (v:v). Accuracy values were calculated by $(a-b)/c$ x100, where a, b and c represent the found amount, original amount and spiked amount, respectively. Analyses were performed in triplicate at each concentration. Analytical method for the precision and accuracy was validated according to the same references as linearity above.

2.8. Cell culture and virus stock

Madin-Darby canine kidney (MDCK) cells were obtained from the American Type Culture Collection (ATCC, Manassas, VA, USA) and maintained in Dulbecco's modified Eagle's medium (DMEM; HyClone, Logan, UT, USA) supplemented with 10% fetal bovine serum (FBS, HyClone), 100 U/mL penicillin and 100 μg/mL streptomycin at 37 °C and 5% CO_2. Avian influenza (H9N2, A/Chicken/Korea/01210/2001) and swine influenza (H1N1, A/PR/8/34) were obtained from Choong Ang Vaccine Laboratory (Daejon, Korea) and their stocks were stored at −80 °C before use (Cho et al., 2019).

2.9. Cytotoxicity assay

The cytotoxicity of the MDCK cells was evaluated using the 3-(4.5-dimethylthiazol-2-yl)-2,5-diphenyltetrazolium bromide (MTT) assay (Huh et al., 2017). MDCK cells were seeded on 96-well plates (1×10^5 cells per well) and maintained for 1 day before use. The cells were washed with phosphate-buffered saline (PBS) and treated with the test compounds of various concentrations. To prevent toxic effects from the solvent, the final concentration of dimethyl sulfoxide (DMSO) in the culture medium was set to 0.05% (v/v). After 48 h of incubation, 20 μL of MTT solution (2 mg/mL) was added to each well, and the samples were incubated for an additional 4 h. The supernatant was carefully removed, and 100 μL of DMSO was added to each well to dissolve the

Table 1
Linearity data, LOD, and LOQ for four active furanocoumarins and their contents in 70% EtOH extract (n = 3).

Compound	Linearity range (μg/injection)	Regression equation	Correlation factor (R)	LOD (μg/injection)	LOQ (μg/injection)	Content (mg/g of extract)
1	0.0156–0.2500	y = 59.233x + 0.071	1.0000	0.0021	0.0063	1.79 ± 0.01
2	0.0625–1.0000	y = 44.072x + 0.211	1.0000	0.0098	0.0298	6.05 ± 0.04
3	0.0078–0.1250	y = 30.686x + 0.023	0.9999	0.0016	0.0048	0.71 ± 0.01
4	0.0625–1.0000	y = 30.337x + 0.159	0.9999	0.0097	0.0293	5.13 ± 0.03

formazan crystals. The optical density was measured at 550 nm. The regression analysis was performed to evaluate the 50% cytotoxic concentration (CC_{50}) using Sigma Plot Statistical Analysis software.

2.10. Cytopathic effect (CPE) inhibition assay

The CPE inhibition assay was performed with a slight modification to a previously reported method (del Barrio et al., 2011). MDCK cells were seeded on 96-well culture plates at a density of 1×10^5 cells per well. After incubation for 24 h, the medium was removed the cells were washed twice with PBS. The influenza H1N1 and H9N2 viruses at a multiplicity of infection (MOI) of 0.01 were inoculated onto near confluent MDCK cell monolayers using DMEM containing 0.15 μg/mL trypsin and 5 μg/mL BSA for 2 h (Huh et al., 2017; Cho et al., 2019). The medium was removed, the cells were washed with PBS, and new medium with several compounds at different concentrations was added. After being incubated for 3 days at 37 °C under a 5% CO_2 atmosphere, the cell medium was replaced with DMEM, 20 μL of 2 mg/mL MTT was added to each well, and the plate was incubated for 4 h at 37 °C. After that, the subsequent steps followed those of the cytotoxicity assay procedures, and the 50% effective concentration (EC_{50}) was evaluated by regression analysis. A selective index (SI) value was determined via formula $SI = CC_{50}/EC_{50}$. The statistical significance was calculated via comparison with the null group.

2.11. Western blotting analysis

The MDCK cell line was grown to approximately 90% spreading in a six-well plate (1 day), and the cells were infected with H1N1 at an MOI of 0.01 and incubated for 2 h. After the medium was changed to DMEM without serum; compounds **1**, **2** and **4** were added at different concentrations. After 24 h of incubation, the cells were washed with chilled PBS, lysed with EBC lysis buffer [1 mM EDTA, 0.5% NP-40, 50 mM NaF, 120 mM NaCl, and 50 mM Tris-HCl (pH 7.6)] and centrifuged for 20 min at 12,000 rpm and 4 °C. Supernatants were collected from the lysates and a protein assay kit (Bio-Rad Laboratories, Inc., Hercules, MA, USA) was used to measure the protein concentrations. Aliquots of lysates were boiled for 5 min and electrophoresed on sodium dodecyl sulfate (SDS)-polyacrylamide gel (10–12% [w/v] acrylamide gel) (Cho et al., 2019). After the proteins were transferred to polyvinylidene fluoride membranes (PVDF 0.45 μm, Immobilon-P, Bedford, MA, USA), the membranes were incubated with primary antibodies: neuraminidase (NA; Gene Tex, San Antonio, TX, USA), nucleoprotein (NP; Novus Biologicals, Littleton, CO, USA), or mouse monoclonal actin (Abcam, Cambridge, UK). The membranes were further incubated with secondary antibodies and detected by a chemiluminescence Western blotting detection kit (Thermo Sci., Waltham, MA, USA) using Image Reader LAS-4000 software (Figs. S6–S9).

2.12. Immunofluorescence assay

The cultures were prepared in a similar manner as those for the Western blot analysis (Cho et al., 2019). After the medium was replaced with new medium containing compounds at the corresponding concentrations, the MDCK Cells were maintained at 37 °C in a CO_2 incubator (5%) for 24 h. After being washed three times with PBS (pH 7.4), the cells were fixed with a 4% paraformaldehyde solution (30 min at room temperature), blocked with 1% BSA (1 h), and then incubated overnight with a monoclonal NP antibody (Novus Biologicals, Littleton, CO, USA) diluted 1:50 in PBS (pH 7.4). After being washed with PBS (pH 7.4), the cells were incubated with a FITC-conjugated goat anti-Rb IgG antibody (Abcam) for 1 h. The cells were then stained with 500 nM DAPI solution for 10 min at room temperature and washed 3 times with PBS (pH 8.0). The slides were mounted with mounting reagent for fluorescence (Vectashield®, Vector Lab, Inc., Burlingame, CA, USA) and imaged by fluorescence microscopy (Olympus ix70, Olympus Corporation, Tokyo, Japan).

2.13. Cell protection assay for H1N1 infection

This assay was performed to observe the effect of preincubation of compound **2** with cells (Theisen and Muller, 2012). MDCK cells were preincubated with compound **2** for 4 h at 37 °C and then infected with H1N1 virus. After 1 h incubation at 37 °C under a 5% CO_2 atmosphere, the monolayers were washed twice with PBS, the medium was replaced with new medium and the cells were incubated for 3 days. The antiviral activity was determined by a cytotoxicity assay.

2.14. Infectivity of H1N1 particles assay

The influenza H1N1 virus was diluted with DMEM containing 0.15 μg/mL trypsin and 5 μg/mL BSA and incubated with or without compound **2** for 1 h at 4 °C (Theisen and Muller, 2012). Then, MDCK cells were incubated with the viral medium for 1 h at 37 °C under 5% CO_2 atmosphere. The cells were washed twice with PBS and incubated for 3 days in new medium. Then, antiviral activity was determined by cytotoxicity assay.

2.15. Neuraminidase inhibition assay

The NA inhibition assay was performed as previously described with several modifications (Dao et al., 2010). Briefly, influenza H1N1 virus was injected into MDCK cells on a large scale using DMEM containing 0.15 μg/mL trypsin and 5 μg/mL BSA. To inactivate viral infectivity, formaldehyde was added to the virus suspension until a final concentration of formaldehyde of approximately 0.1% was reached and then the cells were maintained at 37 °C for 30 min. The NA activity was measured using 4-MU-NANA as the fluorescent substrate. In general, the assay was carried out in 96-well plates containing 10 μL of virus suspensions and 10 μL of tested compounds diluted to the appropriate concentrations in the enzyme buffer (32.5 mM 2-(*N*-morpholino) ethanesulfonic acid with 4 mM $CaCl_2$, pH 6.5). After incubation for 30 min at 37 °C, 30 μL of 4-MU-NANA substrate in enzyme buffer was added into each well. The enzymatic reactions were maintained at 37 °C for 2 h and quenched by treatment with 150 μL of stop solution (25% EtOH, 0.1 M glycine, pH 10.7). Oseltamivir (100 nM) was used as a positive control. The fluorescence of the reaction solution was measured by a SpectraMax GEMNI XPS microplate reader (Molecular Devices, Sunnyvale, CA, USA) with an excitation wavelength of 360 nm and an emission wavelength of 440 nm.

2.16. Molecular docking analysis

Docking studies between polymerase proteins, such as polymerase acidic protein (PA), polymerase basic protein 1 (PB1), and polymerase basic protein 2 (PB2), and compound **2** were successfully performed using Discovery Studio Client v19.1.0.18287/CDOCKER software (Accelrys, San Diego, CA) (Yaeghoobi et al., 2016). The structures of C-terminus of PA, PA-PB1, and PB1-PB2 were obtained from the Protein Data Bank (http://www.pdb.org) (PDB ID code: 3CM8, 2ZNL and 2ZTT, respectively) based on previously reported data (Chang et al., 2015; Watanabe et al., 2017; Li et al., 2013). The structures of the proteins were optimized after the water molecules were deleted, and their binding sites were obtained based on the receptor cavities of each protein. The value of the pose cluster radius was set to 0.5. Protein-ligand binding affinities were optimized and calculated according to the CDOCKER interaction energy arising from several interaction bonds, such as conventional hydrogen bonds, carbon-hydrogen bonds, and π-π T-shaped and π-alkyl interactions.

2.17. Flow cytometric analysis of apoptosis

For the flow cytometry analysis, the cells were prepared in a similar manner as those for quantitative real-time PCR. After 2 days of incubation, the cells were collected from adherent cells and detached cells in the supernatant. After being washed twice with cold PBS, the cells were suspended in cold binding buffer (10 mM HEPES/NaOH pH 7.4, 140 mM NaCl, 2.5 mM $CaCl_2$) at a concentration of 10^6 cells/mL. An ApopNexin™ FITC kit (Chemicon International, Inc., CA, USA) was used in this assay by following the manufacturer's protocol. Briefly, the cell suspension was added to the annexin conjugated with ApopNexin™ FITC and propidium iodide (PI) and incubated in the dark for 15 min at room temperature (Miyamoto et al., 1998). Then, the double-stained cells were immediately analyzed using a flow cytometer (BD FACSCalibur, CA, USA) (Table S1).

2.18. Statistical analysis

Statistical analysis was conducted using one-way analysis of variance with Student's t-test using SPSS ver. 20.0 (SPSS Inc., Chicago, IL, USA). Each experiment was repeated at least three times. All results are shown as the mean ± standard deviation of three independent experiments, and $*p < 0.05$, $**p < 0.01$ and $***p < 0.001$ were considered indicative of statistically significant differences.

3. Results and discussion

3.1. Quantitative analysis of four furanocoumarins isolated from A. dahurica using HPLC-DAD

To quantify the four active furanocoumarins (Fig. 1) in the 70% EtOH extract of *A. dahurica*, an appropriate validation method was established by using HPLC-DAD. Linearity data, including the correlation regression equation, coefficient (*R*), LOD and LOQ, were successfully obtained. The intra- and interday precision and accuracy values were also calculated, and the % relative standard deviation (RSD) values of these assays were less than 5%, indicating that this method was well validated (Table 2). With this quantitative method, the content of the four active compounds was analyzed (Tables 1 and 2), and the results showed that the most abundant was compound 2 (6.05 ± 0.04 mg/g of dried extract), which showed the strongest antiviral activity (Table 3), followed by compounds 4 (5.13 ± 0.03), 1 (1.79 ± 0.01) and 3 (0.71 ± 0.01). A result group reported that the content of imperatorin in 70% ethanolic extract was higher than 7.5 mg/g (Zhang et al., 2017) and another one reported that the contents of isoimperatorin, oxypeucedanin, oxypeucedanin hydrate and imperatorin in 70% methanolic extract were 4.3, 59.0, 2.3 and 6.3 mg/g, respectively (Lee et al., 2015). Although our results showed relatively low contents of four pyranocoumarins, it can be explained, considering that some factors, such as geographical variation in contents and extraction method, can affect the extraction yield. Taken together, considering that the most potent compound predominates among the four compounds and the others also have anti-influenza activity (Table 3), it is likely that compound 2 along with the other three compounds can affect the antiviral activity of the total extract of *A. dahurica*.

3.2. Protective activities of isolated compounds from A. dahurica against the cytopathic effect of the influenza a (H1N1 and H9N2) virus

As a part of our ongoing project to search for new anti-influenza agents from medicinal plants, a 70% EtOH extract of *A. dahurica* was selected for further isolation based on our preliminary experimental results (data not shown). The antiviral activity of compounds isolated from *A. dahurica* was evaluated against influenza A (H1N1 and H9N2) virus by CPE inhibition assay. The cells were treated with four isolated compounds (**1–4**) in a dose-dependent manner to determine the EC_{50}, CC_{50} and SI values. As shown in Table 3, isoimperatorin (**1**) and oxypeucedanin (**2**) exhibited strong antiviral activity, with EC_{50} values (isoimperatorin: 7.67 ± 0.93 μM and 6.72 ± 0.51 μM, respectively/ oxypeucedanin: 5.98 ± 0.71 μM and 4.52 ± 0.39 μM, respectively) comparable to that of ribavirin, whereas the other two compounds showed medium activity against both H1N1 and H9N2. Additionally, decursin, which is the representative pyranocoumarin isolated from *Angelica gigas,* showed no activity against either subtype of influenza A in infected cells, indicating that the shape of the ring attached to the coumarin core structure (in other words, whether it is pyranocoumarin or furanocoumarin) may be a key pharmacophore to inhibit the replication of these viruses. However, to avoid hasty generalization and deduce a clear structure-activity relationship (SAR), these experiments have to be repeated with other pyranocoumarins. Recently, the potential and importance of coumarin as antiviral agent, especially anti-influenza and anti-HIV (human immunodeficiency virus) is emerging. It has been reported that eleutheroside B1, a simple coumarin glycoside, showed anti-influenza activity by inhibiting expression of POLR2A gene which is responsible for the expression of viral polymerase and glycyrol, a benzofuran coumarin isolated from *Glycyrrhiza uralensis*, showed strong NA inhibitory activity with an IC_{50} of 3.1 μM (Mishra et al., 2020). Moreover, another research group has found that angelicin, an angular furanocoumarin, obtained from HTS (high throughput screening) system of about 20,000 compounds exhibited strong anti-influenza activity with an IC_{50} of 4.5 μM and a CC_{50} > 25 μM. This finding encouraged them to perform studies on SAR exploration and finally found the lead optimized compound, a meta-substituted phenyl/ 2-thiophene rings bearing angelicin with 64-fold improved activity (Yeh et al., 2010; Hassan et al., 2016). Since angelicn is one of main active components of *Psoralea corylifolia* and can be found from many plants of Umbelliferae family, the research can be the example of how natural products can be used as a lead compound for the discovery of anti-influenza agent.

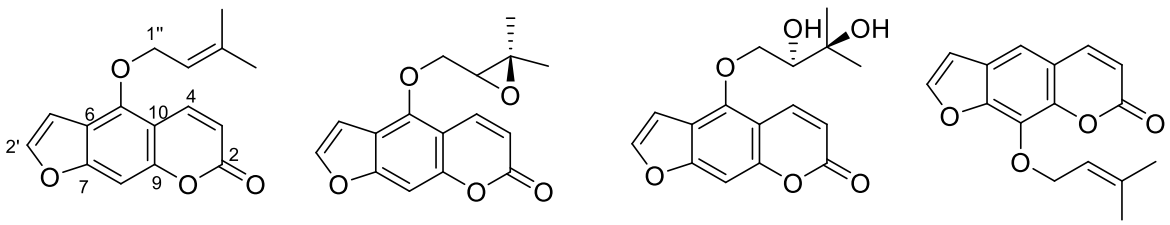

(1) **(2)** **(3)** **(4)**

Fig. 1. Chemical structures of furanocoumarins **1–4** isolated from the roots of *Angelica dahurica*. Isoimperatorin (**1**), oxypeucedanin (**2**), oxypeucedanin hydrate (**3**) and imperatorin (**4**).

Table 2
Precision and accuracy data of each analyte determined by standard addition method (n = 3).

Compound	Precision			Accuracy				
	Concentration (μg/injection)	Intra day precision (% RSD)	Inter day precision (% RSD)	Original amount (μg/injection)	Spiked amount (μg/injection)	Found amount (μg/injection)	Recovery[a] (%)	RSD (%)
1	0.2500	0.1	2.0	0.0893	0.0938	0.1869 ± 0.0020	105.2	2.0
	0.1250	0.3	3.5	0.0893	0.0625	0.1515 ± 0.0013	100.5	2.1
	0.0313	0.1	3.5	0.0893	0.0313	0.1204 ± 0.0010	100.5	3.2
2	1.0000	0.1	0.3	0.3024	0.3750	0.6889 ± 0.0050	107.0	1.3
	0.5000	0.3	1.8	0.3024	0.2500	0.5477 ± 0.0050	101.9	2.0
	0.1250	0.1	1.8	0.3024	0.1250	0.4252 ± 0.0035	102.0	2.9
3	0.1250	0.2	2.7	0.0355	0.0469	0.0844 ± 0.0008	105.6	1.5
	0.0625	1.1	2.0	0.0355	0.0313	0.0664 ± 0.0007	100.0	2.1
	0.0156	0.4	0.8	0.0355	0.0156	0.0507 ± 0.0004	98.6	2.4
4	1.0000	0.1	0.8	0.2565	0.3750	0.6446 ± 0.0037	104.6	1.0
	0.5000	0.3	2.4	0.2565	0.2500	0.5039 ± 0.0053	100.0	2.1
	0.1250	0.1	2.4	0.2565	0.1250	0.3829 ± 0.0029	102.2	2.4

[a] Purities of each compound were taken into consideration for the clarity.

3.3. Inhibitory effects of compounds isolated from A. dahurica on the expression of viral proteins

As it is obviously well studied, influenza infection and replication is a multistep process, including penetration of a virion, transcription/replication of viral RNA, assembly of viral proteins, and release of a virus progeny (Shie and Fang, 2019). Therefore, we performed various assays to investigate on which steps active compounds have influence on. Since compound **2** showed the strongest activity in the CPE inhibition assay and predominates among four compounds in the total extract, we selected compound **2** and performed a compound treatment timecourse assay with H1N1 virus to determine which stages of the viral replication cycle are disturbed by compound **2** (Theisen and Muller, 2012). In brief, the MDCK cells were treated with compound **2** (40 μM) or ribavirin (40 μM) at different time points after H1N1 virus infection (1 h−12 h). As shown in Fig. 2A, when MDCK cells were treated with compound **2** 1 h postinfection, the inhibitory activity was approximately 80–90%. However, the inhibition effect decreased to less than 40% when cells were treated with compound **2** 6 h postinfection. Furthermore, the results indicated that compound **2** and ribavirin showed similarly strong inhibition patterns from 1 h to 3 h postinfection groups. However, compound **2** treated group showed gradually decreasing pattern from 3 h to 8 h postinfection groups, whereas cell viability in the ribavirin treated group drastically decreased in 3 h–5 h. Considering that ribavirin inhibits the early phase of viral replication in host cells (Browne, 1979; Wang et al., 2011a) and this comparative result, it is likely that compound **2** has inhibitory effects on several target points, mainly early phase of viral cycle, whereas activity of ribavirin mostly focuses on early phase.

According to accumulative studies about influenza virus, viral proteins synthesis (or expression) is the important step in the early phase of viral replication and, especially the synthesis of NP is considered an indication of early viral protein synthesis (Abdoli et al., 2013; Banerjee et al., 2013). Actually, mRNA synthesis occurs earlier than complementary RNA (cRNA) and viral RNA (vRNA) transcription by the aid of primers. The initial mRNA transcription consequently leads to synthesis of polymerase subunits (PA, PB1, and PB2) and NP that are imported back into the nucleus and used for the synthesis of newly formed complementary ribonucleoproteins (cRNPs) and progeny vRNPs (Dou et al., 2018). Therefore, we decided to perform a Western blot assay at certain compound treatment time points postinfection (2, 6, 12 and 18 h after infection) to see whether compound **2** inhibits the synthesis of viral protein, especially NP and NA in the early phase of viral replication cycle. The results in Fig. 2B showed that compared to the treatment point at 18 h of NA and NP, the production levels of both viral proteins significantly decreased to less than 20% in the cells treated with compound **2** (20 μM) 2 h after infection (Fig. S6). This expression inhibition tendency was inversely proportional to the treatment onset time after infection. Considering that vRNPs enter the nucleus of the host cell from the cell surface in approximately 1 h and that NP and NA play major roles in replication of the vRNPs and viral release, respectively (Dou et al., 2018), these results can explain the CPE inhibitory pattern of compound **2** in Fig. 2A and that compound **2** exerts its anti-influenza activity via inhibition of synthesis of NP and NA. This observation is repeatedly shown in another Western blot assay, showing that compound **2** significantly reduced the levels of NA and NP in a dose-dependent manner at concentrations of 20, 10, 5.0 and 2.0 μM (Figs. 2C and S7). Furthermore, the results in Fig. 2C were clearly supported by an immunofluorescence assay. The host cells were infected with H1N1 for 2 h and then the cells were treated with compound **2** and ribavirin as a positive control. After incubation at 37 °C for 24 h, the expression of NP was detected by using an

Table 3
Protective effects of compounds isolated from *A. dahurica* against H1N1 and H9N2.

Condition	CC_{50} (μM)	EC_{50} (μM)		SI (= CC_{50}/EC_{50})	
		H1N1	H9N2	H1N1	H9N2
1	114.02 ± 11.10	7.67 ± 0.93	6.72 ± 0.51	14.87 ± 0.31	16.97 ± 0.34
2	101.37 ± 9.75	5.98 ± 0.71	4.52 ± 0.39	16.95 ± 0.34	22.43 ± 0.20
3	> 200	10.50 ± 0.67	10.50 ± 1.29	> 19.05 ± 1.14	> 18.69 ± 2.01
4	104.62 ± 8.59	11.31 ± 0.46	8.10 ± 0.48	9.25 ± 0.37	12.91 ± 0.28
Decursin	> 200	N.A.[b]	N.A.[b]	–	–
Oseltamivir[a]	> 200	0.49 ± 0.06	0.33 ± 0.08	> 414.38 ± 44.53	> 643.90 ± 118.26
Ribavirin[a]	> 200	6.29 ± 0.89	6.13 ± 0.19	> 32.45 ± 3.94	> 32.67 ± 1.04

[a] Positive control.
[b] N.A. = No activity.

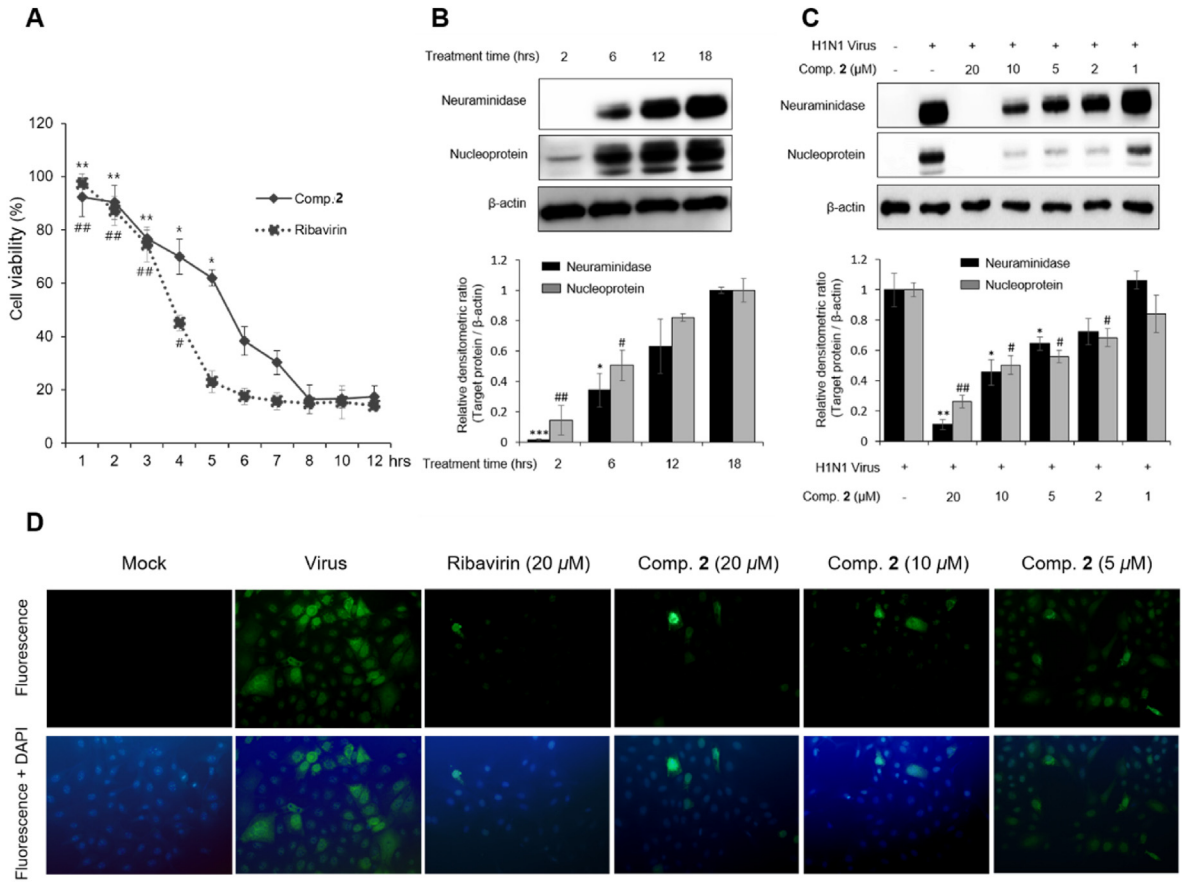

Fig. 2. Inhibitory effects of compound **2** on the influenza viral cycle. (**A**) The virus-infected cells were treated with compound **2** or ribavirin (40 μM) at different time points. After 3 days of incubation, the antiviral activity was evaluated using a CPE inhibition assay. The results are shown as the mean ± SD ($n = 2$); $^{*}p < 0.05$ and $^{**}p < 0.01$ compared to the virus-infected control. (**B**) Likewise, Western blot analysis revealed that compound **2** (20 μM) inhibits NA and NP production during different phases of the influenza virus replication cycle. Data are shown as the mean ± SD ($n = 2$); $^{*}p < 0.05$ and $^{***}p < 0.001$ compared to the treatment point at 18 h of NA; $^{\#}p < 0.05$ and $^{\#\#}p < 0.01$ compared to treatment point at 18 h of NP. (**C**) Dose-dependent inhibitory effects of compound **2** on viral protein synthesis. The virus-infected cells were treated with different concentrations of compound **2**. After 24 h of incubation, NA and NP levels were determined using Western blot analysis. The results are expressed as the mean ± SD ($n = 2$); $^{*}p < 0.05$ and $^{**}p < 0.01$ compared to the virus-infected control of NA; $^{\#}p < 0.05$ and $^{\#\#}p < 0.01$ compared to the virus-infected control of NP. (**D**) The influence of compound **2** on protein expression was investigated using an immunofluorescence assay. MDCK cells were infected with H1N1 for 2 h and then treated with compound **2** and ribavirin as a positive control. After being incubated at 37 °C for 24 h, the cells were fixed with paraformaldehyde and the expression of NP was detected by immunofluorescence.

immunofluorescence assay. As shown in Fig. 2D, the green fluorescence of NP was detected in the cytoplasm and nucleus of the virus-infected cells not treated with a compound, whereas fluorescence was not found in noninfected cells. However, when virus-infected cells were treated with ribavirin (20 μM) or compound **2** at different concentrations (20, 10, and 5.0 μM), the number of cells expressing NPs was significantly decreased in a dose-dependent manner. Therefore, these results suggest that compound **2** might have potential activity against the production of cRNPs and progeny vRNPs via inhibiting the synthesis of NP and against the release of progeny virus via inhibiting the synthesis of NA, although the specific intracellular targets need to be determined.

*3.4. Effects of compound **2** on host cells, H1N1 virus or neuraminidase activity*

In addition to the observations found in Fig. 2, additional assays were performed to investigate the effects of compound **2** on host cells, virus or neuraminidase activity. Firstly, protective effect of compound **2** against H1N1 virus infection was evaluated. MDCK cells were pre-incubated with compound **2** at concentrations of 20, 10 and 5.0 μM for 4 h before virus infection, followed by 3 days of incubation. The data in Fig. 3A indicates that pretreatment with compound **2** did not exhibit statistically significant increase of cell viability in any concentrations, which means compound **2** does not have any effects on host cells to prevent virus entry. Next, a direct virucidal effect of compound **2** was assessed by similar manner as those for the experiments in Fig. 3A. Preincubation of H1N1 virus with compound **2** at concentrations of 20, 10 and 5.0 μM at 4 °C for 1 h before viral infection also did not change the cell viability compared to the untreated control, indicating compound **2** can't deactivate or destroy the virus (Fig. 3B). Furthermore, a direct inhibitory activity of compound **2** on the release of replicated viruses via the interaction with the NA was also assessed using NA inhibition assay. As shown in Fig. 3C, compound **2** at any concentrations did not inhibit NA, which is another important virulence factor of influenza infection. Overall, these data clarified that compound **2** exhibited its anti-influenza activity not by inhibiting virus entry, release, and neuraminidase activity but by restraining the synthesis of NP and NP.

3.5. Docking analysis

With the aforementioned results showing that compound **2** likely exhibits anti-influenza activity in the early phase of the viral replication cycle by inhibiting the expression of viral proteins, molecular docking analysis was performed to predict the binding affinity between compound **2** and viral RNA polymerase which is important anti-influenza

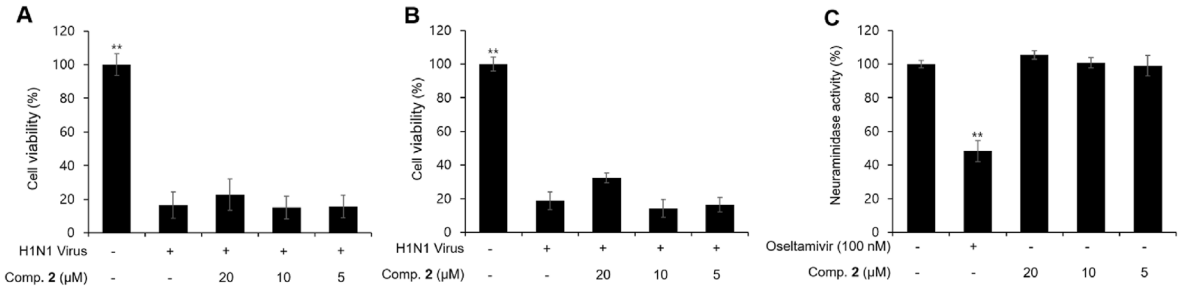

Fig. 3. Mechanistic studies of compound **2** against influenza A virus. (**A**) MDCK cells were preincubated with compound **2** at concentrations of 20, 10 and 5.0 μM for 4 h before virus infection. After 3 days of incubation, the antiviral activity was evaluated using a CPE inhibition assay. Data are expressed as the mean ± SD (n = 2); $^{**}p < 0.01$ compared to the virus-infected control. (**B**) Preincubation of virus in DMEM medium with compound **2** (20, 10 and 5.0 μM) at 4 ˚C for 1 h. Then, MDCK cells were incubated with the viral medium for 1 h at 37 ˚C under 5% CO_2 atmosphere. The CPE inhibition assay was performed after 3 days of incubation. Data are expressed as the mean ± SD (n = 2); $^{**}p < 0.01$ compared to the virus-infected control. (**C**) The effect of compound **2** on the release of new virions via the interaction with the NA binding site was determined by an NA inhibition assay. Data are expressed as the mean ± SD (n = 2); $^{**}p < 0.01$ compared to the negative control.

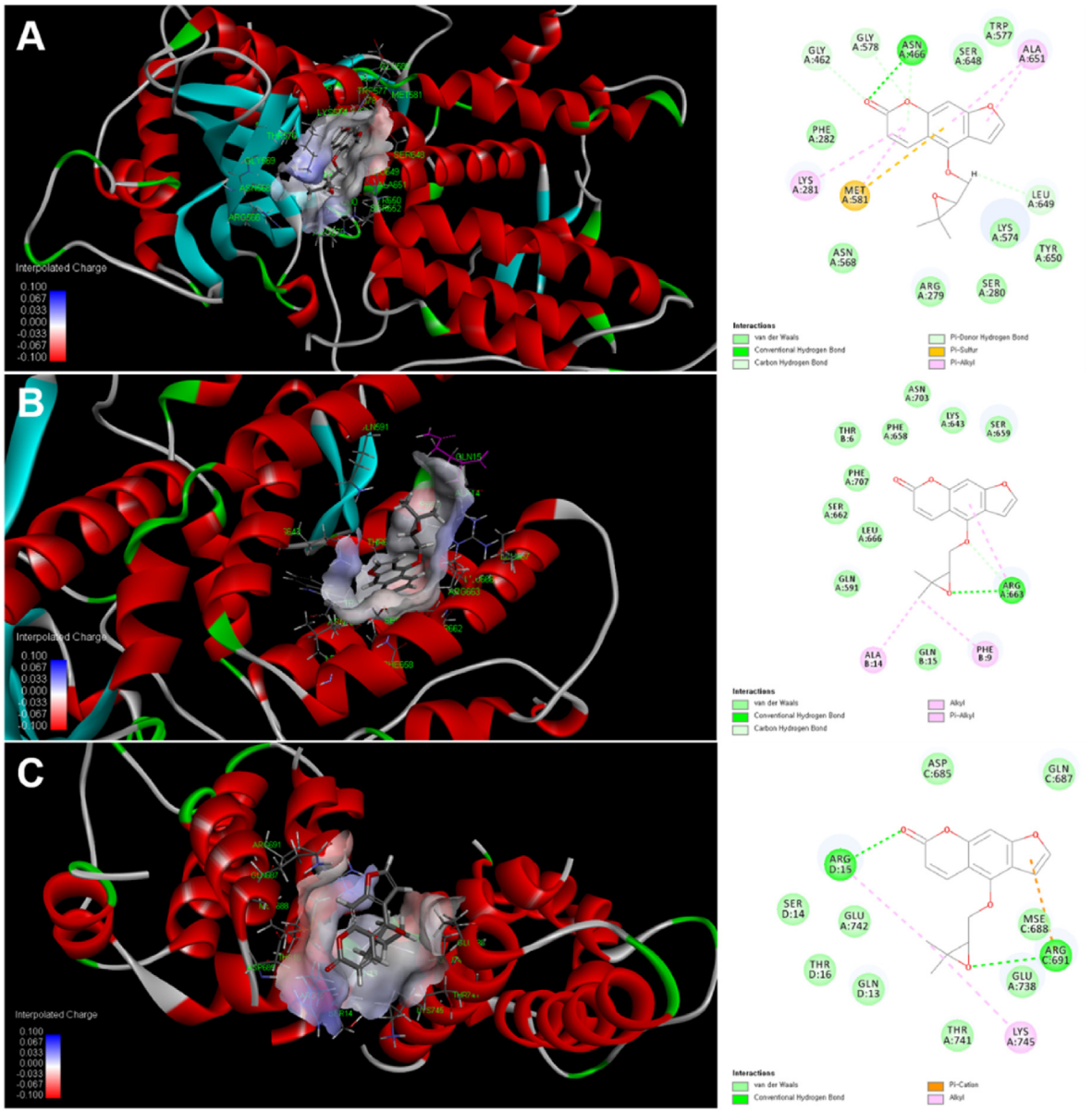

Fig. 4. Illustration of the molecular docking simulation and 2D diagram of the interactions between polymerase proteins, such as PA, PB1 and PB2, and compound **2** using Discovery Studio Client v19.1.0.18287/CDOCKER software. The structures of the C-terminus of PA (**A**), PA-PB1 (**B**), and PB1-PB2 (**C**) were obtained from the Protein Data Bank (http://www.pdb.org) (PDB ID code: 3CM8, 2ZNL and 2ZTT, respectively) based on previously reported data (Chang et al., 2015; Watanabe et al., 2017; Li et al., 2013).

target for drug discovery. The RNA-dependent RNA polymerase (RdRp) of influenza A is composed of three subunits, PA, PB1, and PB2 (Chang et al., 2015). They play a crucial role in mRNA/vRNA transcription and have their own distinct parts for that. PB1 subunit is the place where cRNA is elongated through the formation of an A-G dinucleotide in cRNA transcription (Dou et al., 2018). Also, for cap snatching which is an essential step for mRNA transcription, influenza virus uses PB2 subunit to bind 5′ cap of a host mRNA and endonuclease domain in the PA subunit to cleave nucleotides of the 5' cap (Guilligay et al., 2008; Dias et al., 2009). Therefore, molecular docking analysis of compound **2** to the active site of these three subunits was performed based on previously reported data (Watanabe et al., 2017; Li et al., 2013). As shown in Fig. 4A, the carbonyl carbon forms a conventional hydrogen bond with ASN466, and the rich aromaticity of compound **2** enables π-alkyl and π-sulfur interactions with the surrounding amino acid residues of the C-terminus of PA (PAC), such as ALA651, LYS281 and MET581. The CDOCKER interaction energy was calculated to be −36.28 kcal/mol. In the interaction with the PA-PB1 complex, a reduced binding affinity was observed (−29.29 kcal/mol), and the oxygen atom in the dimethyl oxirane moiety of the structure formed a conventional hydrogen bond with ARG663 of PAC (residues 257–716), whereas a methyl group formed π-alkyl interaction with ALA14 and PHE9 of the PB1 (residues 1–25 and 680–759) subunit (Fig. 4B), indicating that compound **2** may disrupt the interaction between PAC and PB1 subunits (Muratore et al., 2012). The interaction with the PB1-PB2 complex showed the lowest binding affinity, −21.86 kcal/mol, and oxygen atoms in the dimethyl oxirane moiety and carbonyl group formed conventional hydrogen bonds with PB1 ARG691 and ARG15, whereas the furan ring showed π-cation interaction with ARG691 (Fig. 4C). In addition, the rate of docking success differed in the three trials. In the first case, molecular docking of compound **2** into PAC was successful in 5 out of 20 active sites with similar values, whereas the other two trials had 2 successes out of 14 sites and 1 success out of 7 sites. Taken together, these findings suggest that there is a possibility that the major target of compound **2** is on the PAC domain rather than the other subunits, affecting mRNA transcription. If this hypothesis is confirmed by further *in vitro* mechanistic studies, it will have great potential as a therapeutic agent, as the PA subunit has potential active sites, including an endonuclease, and the structure of the PA subunit is conserved across type A, B and C influenza viruses, which makes PA a promising target for most influenza strains with reduced susceptibility to drug resistance (Li et al., 2012).

3.6. Inhibitory effect of compound 2 on apoptosis during influenza virus propagation in MDCK cells

Programmed cell death termed "apoptosis" is an important defensive immune reaction induced during viral infection to limit viral dissemination by removing unwanted cells. However, many viruses, including influenza A virus, abuse apoptosis for their own benefit to evade and subvert host cells, and it is scientifically regarded as a hallmark event upon infection with many viral pathogens (Yeganeh et al., 2018; Fujikura and Miyazaki, 2018). In particular, influenza virus has been reported to induce apoptosis by causing DNA fragmentation both *in vitro* and *in vivo* (Takizawa et al., 1993; Mori et al., 1995; Hinshaw et al., 1994). Thus, the inhibition of apoptosis during viral infection is also a crucial target for anti-influenza agent discovery. Based on the effects of isolated compounds, especially compound **2**, on the viral replication and multiplication of influenza virus, the inhibitory effect of **2** on apoptosis during viral infection was also evaluated. Flow cytometric analysis was performed to detect apoptosis using an annexin conjugate ApopNexin^{TM} FITC kit, and the total number of apoptotic cells included early apoptotic cells and late apoptotic cells. As shown in Fig. 5A–C, the number of apoptotic cells increased significantly in virus-infected cells (34.16%) compared to uninfected cells (4.12%). However, when the viral-infected cells were coincubated with compound **2** (20 μM), the proportion of apoptotic cells decreased markedly to 12.84%. This result indicates that compound **2** has an antiapoptotic effect on influenza A virus-induced apoptosis in host cells.

To confirm the above results, the effect of compound **2** on the mRNA expression of caspase-3 and Box, which are essential proteins for viral replication and propagation that function by inducing apoptosis (Wurzer et al., 2003; McLean et al., 2009), was also evaluated by using real-time PCR. In brief, MDCK cells were infected with H1N1 virus for 2 h and then treated with or without compound **2** at different concentrations. After 24 h of incubation, a real-time PCR assay was carried out to analyze the expression of these genes. The results in Fig. 5D show that compound **2** significantly decreased the mRNA expression of caspase-3 and Bax protein in a dose-dependent manner at concentrations of 20, 10, and 5.0 μM.

4. Conclusion

In our continuous efforts to find promising anti-influenza agents, bioactivity-guided isolation was performed to isolate four representative active furanocoumarins from the active 70% EtOH extract of *A. dahurica*. These four isolates were found to have dose-dependent CPE inhibition activity against H1N1 and H9N2. Of the compounds, as compound **2** exhibited the strongest activity in both subtypes, it was subjected to detailed mechanistic studies. Compound **2** was shown to exert its anti-influenza activity by disturbing synthesis of NP and NA in the early phase of viral replication cycle but not affecting virus entry into host cells, virus budding and release, or not the virucidal activity. According to the results above, *in silico* molecular docking analysis was performed to predict the binding affinity of compound **2** for polymerase subunits. The molecular docking analysis indicated that compound **2** is likely to act on PAC, resulting in the inhibition of viral mRNA transcription and subsequent viral protein synthesis. In addition, compound **2** reduced the H1N1-induced apoptosis of cells by inhibiting the Bax/casepase-3 pathway. Therefore, we provide evidence for the ethnopharmacological use of *A. dahurica* as a common cold and flu remedy and the potential of compound **2** as an anti-influenza agent. Currently, as individual action is not sufficient to minimize the damage caused by a pandemic (or endemic), multidisciplinary measures including the development of food additives increasing immunity, vaccine development and strict biosecurity, have to be implemented when influenza virus pandemics break out to efficiently reduce mortality and morbidity. Our findings suggest that the extract of *A. dahurica* has potential as a food additive to raise body's resistance to influenza infection, and the isolated furanocoumarins are lead compounds.

Author contributions

Ba Wool Lee (paul36@snu.ac.kr).

- performed quantitative analysis, validation and molecular docking analysis of compounds and wrote the manuscript.

Thi Kim Quy Ha (htkquy@ctu.edu.vn).

- designed and performed biological experiments.

Hyo Moon Cho (chgyand@naver.com) and Jin-Pyo An (ntopjp77@gmail.com).

- aided fractionation, isolation and characterization of compounds from *A. dahurica*.

Seong Kyun Kim (k2s013@cavac.co.kr) and Choong-Sik Kim (okkings@cavac.co.kr).

- purified and provided virus stocks of two subtypes of influenza virus.

Eunhee Kim (ehkim@cavac.co.kr).

-supervised the all process of purification and supply of virus stock.

Won Keun Oh (wkoh1@snu.ac.kr).

- designed the whole process of the research as a corresponding author.

The manuscript was reviewed by all authors.

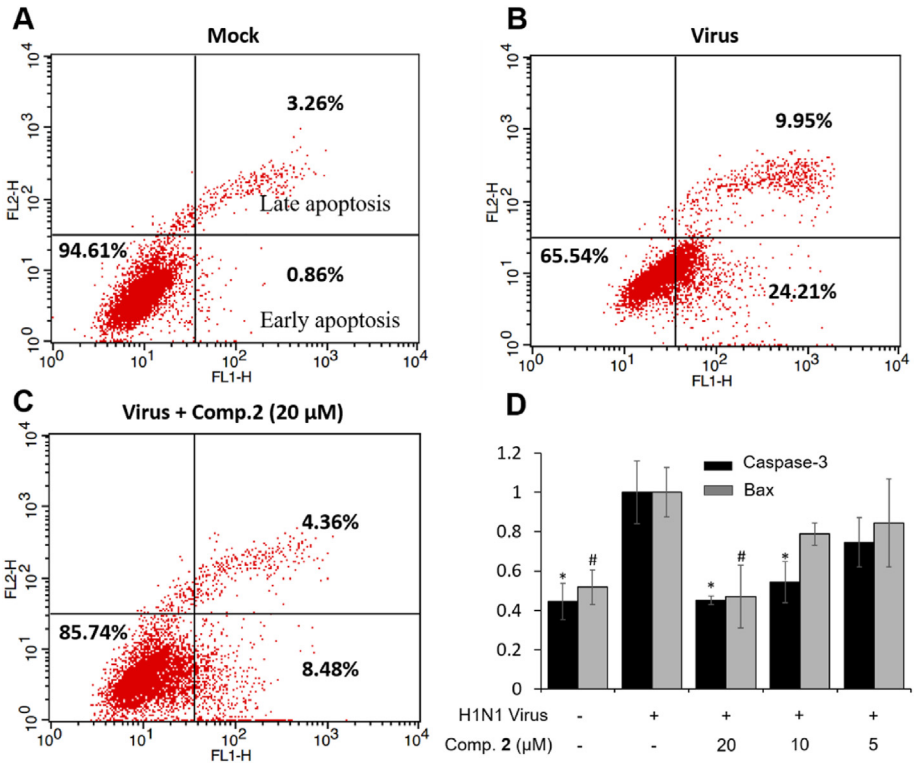

Fig. 5. The inhibitory effects of compound **2** on apoptosis during H1N1 virus infection of MDCK cells. (**A-C**) The virus-infected cells were treated with compound **2** (20 μM) and incubated for 2 days. After that, flow cytometric analysis was performed to detect apoptosis using an ApopNexin^{TM} FITC kit, and the total number of apoptotic cells included early apoptotic cells and late apoptotic cells. (**D**) The effects of compound **2** on the expression of genes encoding caspase-3 and Bax proteins. The virus-infected cells were exposed to compound **2** at different concentrations. Real-time PCR assays were carried out to analyze the expression of these genes after 24 h of incubation. The results are expressed as the mean ± SD (n = 2); $^{*}p$ < 0.05 compared to the virus-infected control of caspase-3; $^{\#}p$ < 0.05 compared to the virus-infected control of Bax.

Funding

This work was supported financially by grants from the Korea Bioactive Natural Material Bank (NRF-2017M3A9B8069409) of the National Research Foundation of Korea (NRF) which is funded by the Ministry of Science and ICT and the Korea Institute of Planning and Evaluation for Technology in Food, Agriculture and Forestry (IPET) through the Animal Disease Management Technology Development Program funded by the Ministry of Agriculture, Food and Rural Affairs (MAFRA) (318031031SB010).

Declaration of competing interest

All authors declare that they have no conflict of interest regarding this study.

Appendix A. Supplementary data

Supplementary data to this article can be found online at https://doi.org/10.1016/j.jep.2020.112945.

References

Abdoli, A., Soleimanjahi, H., Tavassoti Kheiri, M., Jamali, A., Jamaati, A., 2013. Determining influenza virus shedding at different time points in madin-darby canine kidney cell line. Cell J 15 (2), 130–135.
An, J.P., Choi, J.H., Huh, J., Lee, H.J., Han, S., Noh, J.-R., Kim, Y.-H., Lee, C.-H., Oh, W.-K., 2019. Anti-hepatic steatosis activity of Sicyos angulatus extract in high-fat diet-fed mice and chemical profiling study using UHPLC-qTOF-MS/MS spectrometry. Phytomedicine 63, 152999.
Banerjee, I., Yamauchi, Y., Helenius, A., Horvath, P., 2013. High-content analysis of sequential events during the early phase of influenza A virus infection. PloS One 8 (7), e68450.
Bergendorff, O., Dekermendjian, K., Nielsen, M., Shan, R., Witt, R., Ai, J., Sterner, O., 1997. Furanocoumarins with affinity to brain benzodiazepine receptors in vitro. Phytochemistry 44 (6), 1121–1124.
Browne, M.J., 1979. Mechanism and specificity of action of ribavirin. Antimicrob. Agents Chemother. 15 (6), 747–753.
Chang, S., Sun, D., Liang, H., Wang, J., Li, J., Guo, L., Wang, X., Guan, C., Boruah, B.M., Yuan, L., Feng, F., Yang, M., Wang, L., Wang, Y., Wojdyla, J., Li, L., Wang, J., Wang, M., Cheng, G., Wang, H.-W., Liu, Y., 2015. Cryo-EM structure of influenza virus RNA polymerase complex at 4.3 Å resolution. Mol. Cell 57 (5), 925–935.
Cho, H.M., Doan, T.P., Ha, T.K.Q., Kim, H.W., Lee, B.W., Pham, H.T.T., Cho, T.O., Oh, W.K., 2019. Dereplication by high-performance liquid chromatography (HPLC) with quadrupole-time-of-flight mass spectroscopy (qTOF-MS) and antiviral activities of phlorotannins from Ecklonia cava. Mar. Drugs 17 (3), 149.
Choi, I.-H., Song, Y.-K., Lim, H.-H., 2008. Analgesic and anti-inflammatory effect of the aqueous extract of Angelica dahurica. J. Korean Oriental Med. 29 (2), 32–40.
Dao, T.T., Tung, B.T., Nguyen, P.H., Thuong, P.T., Yoo, S.S., Kim, E.H., Kim, S.K., Oh, W.K., 2010. C-methylated flavonoids from Cleistocalyx operculatus and their inhibitory effects on novel influenza A (H1N1) neuraminidase. J. Nat. Prod. 73 (10), 1636–1642.
del Barrio, G., Spengler, I., García, T., Roque, A., Álvarez, A.L., Calderón, J.S., Parra, F., 2011. Antiviral activity of Ageratina havanensis and major chemical compounds from the most active fraction. Br. J. Pharmacol. 21 (5), 915–920.
Dias, A., Bouvier, D., Crépin, T., McCarthy, A.A., Hart, D.J., Baudin, F., Cusack, S., Ruigrok, R.W., 2009. The cap-snatching endonuclease of influenza virus polymerase resides in the PA subunit. Nature 458 (7240), 914–918.
Dou, D., Revol, R., Östbye, H., Wang, H., Daniels, R., 2018. Influenza A virus cell entry, replication, virion assembly and movement. Front. Immunol. 9, 1581.
Eng, Y.S., Lee, C.H., Lee, W.C., Huang, C.C., Chang, J.S., 2019. Unraveling the molecular mechanism of traditional Chinese medicine: formulas against acute airway viral infections as examples. Molecules 24 (19), E3505.
Fujikura, D., Miyazaki, T., 2018. Programmed cell death in the pathogenesis of influenza. Int. J. Mol. Sci. 19 (7), 2065.
Gilani, A.H., Rahman, A., 2005. Trends in ethnopharmacology. J. Ethnopharmacol. 100 (1–2), 43–49.
Guilligay, D., Tarendeau, F., Resa-Infante, T., Coloma, R., Crepin, T., Sehr, P., Lewis, J., Ruigrok, R.W., Ortin, J., Hart, D.J., Cusack, S., 2008. The structural basis for cap binding by influenza virus polymerase subunit PB2. Nat. Struct. Mol. Biol. 15 (5), 500–506.
Harkar, S., Razdan, T.K., Waight, E.S., 1984. Steroids, chromone and coumarins from Angelica officinalis. Phytochemistry 23 (2), 419–426.
Hassan, M.Z., Osman, H., Ali, M.A., Ahsan, M.J., 2016. Therapeutic potential of coumarins as antiviral agents. Eur. J. Med. Chem. 123, 236–255.
Hinshaw, V.S., Olsen, C.W., Dybdahl-Sissoko, N., Evans, D., 1994. Apoptosis: a mechanism of cell killing by influenza A and B viruses. J. Virol. 68 (6), 3667–3673.
Huh, J., Ha, T.K.Q., Kang, K.B., Kim, K.H., Oh, W.K., Kim, J., Sung, S.H., 2017. C-methylated flavonoid glycosides from Pentarhizidium orientale rhizomes and their inhibitory effects on the H1N1 influenza virus. J. Nat. Prod. 80 (10), 2818–2824.
ICH, T.Q.B., 1996. Guidance for Industry, Q2B Validation of Analytical Procedures. Methodology. FDA, Rockville.
Jin, S.E., Ha, H., Jeong, S.-J., Shin, H.-K., 2014. Effects of Korean traditional herbal formula for common cold on the activities of human CYP450 isozymes. J. Korean Med. 35 (2), 47–59.
Kang, O.H., Lee, G.H., Choi, H.J., Park, P.S., Chae, H.S., Jeong, S.I., Kim, Y.C., Sohn, D.H., Park, H., Lee, J.H., Kwon, D.Y., 2007. Ethyl acetate extract from Angelica Dahuricae Radix inhibits lipopolysaccharide-induced production of nitric oxide, prostaglandin

E_2 and tumor necrosis factor-α via mitogen-activated protein kinases and nuclear factor-κB in macrophages. Pharmacol. Res. 55 (4), 263–270.
Kim, H.S., Chi, H.-J., 1990. Studies on essential oils of plants of Angelica genus in Korea (III). Essential oils of Angelicae dahuricae Radix. Korean J. Pharmacogn. 21 (2), 121–125.
Koziol, E., Skalicka-Woźniak, K., 2016. Imperatorin-pharmacological meaning and analytical clues: profound investigation. Phytochemistry Rev. 15, 627–649.
Kurokawa, M., Tsurita, M., Brown, J., Fukuda, Y., Shiraki, K., 2002. Effect of interleukin-12 level augmented by Kakkon-to, a herbal medicine, on the early stage of influenza infection in mice. Antivir. Res. 56 (2), 183–188.
Lee, K., Shin, M.S., Ham, I., Choi, H.-Y., 2015. Investigation of the mechanisms of Angelica dahurica root extract-induced vasorelaxation in isolated rat aortic rings. BMC Compl. Alternative Med. 15, 395.
Li, C., Ba, Q., Wu, A., Zhang, H., Deng, T., Jiang, T., 2013. A peptide derived from the C-terminus of PB1 inhibits influenza virus replication by interfering with viral polymerase assembly. FEBS J. 280 (4), 1139–1149.
Li, D., Wu, L., 2017. Coumarins from the roots of Angelica dahurica cause anti-allergic inflammation. Exp. Ther. Med. 14 (1), 874–880.
Li, L., Chang, S., Xiang, J., Li, Q., Liang, H., Tang, Y., Liu, Y., 2012. Screen anti-influenza lead compounds that target the PAc subunit of H5N1 viral RNA polymerase. PloS One 7 (8), e35234.
Liu, H., Lai, H., Jia, X., Liu, J., Zhang, Z., Qi, Y., Zhang, J., Song, J., Wu, C., Zhang, B., Xiao, P., 2013. Comprehensive chemical analysis of Schisandra chinensis by HPLC–DAD–MS combined with chemometrics. Phytomedicine 20 (12), 1135–1143.
Lu, X., Yuan, Z.Y., Yan, X.J., Lei, F., Jiang, J.F., Yu, X., Yang, X.W., Xing, D.M., Du, L.J., 2016. Effects of Angelica dahurica on obesity and fatty liver in mice. Chin. J. Nat. Med. 14 (9), 641–652.
Luo, K.W., Sun, J.G., Chan, J.Y., Yang, L., Wu, S.H., Fung, K.P., Liu, F.Y., 2011. Anticancer effects of imperatorin isolated from Angelica dahurica: induction of apoptosis in HepG2 cells through both death-receptor- and mitochondria-mediated pathways. Chemotherapy 57 (6), 449–459.
McLean, J.E., Datan, E., Matassov, D., Zakeri, Z.F., 2009. Lack of Bax prevents influenza A virus-induced apoptosis and causes diminished viral replication. J. Virol. 83 (16), 8233–8246.
Mishra, S., Pandey, A., Manvati, S., 2020. Coumarin: an emerging antiviral agent. Heliyon 6 (1), e03217.
Miyamoto, D., Kusagaya, Y., Endo, N., Sometani, A., Takeo, S., Suzuki, T., Arima, Y., Nakajima, K., Suzuki, Y., 1998. Thujaplicin-copper chelates inhibit replication of human influenza viruses. Antivir. Res. 39 (2), 89–100.
Moon, Y.H., Go, J.J., Park, J.Y., 1999. The anti-inflammatory and analgesic activities of Gumiganghwaltang. Korean J. Pharmacogn. 30 (1), 18–24.
Mori, I., Komatsu, T., Takeuchi, K., Nakakuki, K., Sudo, M., Kimura, Y., 1995. In vivo induction of apoptosis by influenza virus. J. Gen. Virol. 76, 2869–2873.
Muratore, G., Goracci, L., Mercorelli, B., Foeglein, Á., Digard, P., Cruciani, G., Palù, G., Loregian, A., 2012. Small molecule inhibitors of influenza A and B viruses that act by disrupting subunit interactions of the viral polymerase. Proc. Natl. Acad. Sci. U.S.A. 109 (16), 6247–6252.
Park, K.J., Lee, H.H., 2005. In vitro antiviral activity of aqueous extracts from Korean medicinal plants against influenza virus type A. J. Microbiol. Biotechnol. 15 (5), 924–929.
Pervin, M., Hasnat, M.A., Debnath, T., Park, S.R., Kim, D.H., Lim, B.O., 2014. Antioxidant, anti-inflammatory and antiproliferative activity of Angelica dahurica root extracts. J. Food Biochem. 38 (3), 281–292.
Sarker, S.D., Nahar, L., 2004. Natural medicine: the genus Angelica. Curr. Med. Chem. 11 (11), 1479–1500.
Shie, J.-J., Fang, J.-M., 2019. Development of effective anti-influenza drugs: congeners and conjugates – a review. J. Biomed. Sci. 26 (1), 1–20.
Shokoohinia, Y., Sajjadi, S.E., Gholamzadeh, S., Fattahi, A., Behbahani, M., 2014. Antiviral and cytotoxic evaluation of coumarins from Prangos ferulacea. Pharm. Biol. 52 (12), 1543–1549.
Takizawa, T., Matsukawa, S., Higuchi, Y., Nakamura, S., Nakanishi, Y., Fukuda, R., 1993. Induction of programmed cell death (apoptosis) by influenza virus infection in tissue culture cell. J. Gen. Virol. 74, 2347–2355.
Tavakoli, S., Delnavazi, M.-R., Hadjiaghaee, R., Jafari-Nodooshan, S., Khalighi-Sigaroodi, F., Akhbari, M., Hadjiakhoondi, A., Yassa, N., 2018. Bioactive coumarins from the roots and fruits of Ferulago trifida Boiss., an endemic species to Iran. Nat. Prod. Res. 32 (22), 2724–2728.
Theisen, L.L., Muller, C.P., 2012. EPs® 7630 (Umckaloabo®), an extract from Pelargonium sidoides roots, exerts anti-influenza virus activity in vitro and in vivo. Antivir. Res. 94 (2), 147–156.
Tun, T., Kang, Y.S., 2017. Imperatorin is transported through blood-brain barrier by carrier-mediated transporters. Biomol. Ther. 25 (4), 441–451.
Walasek, M., Grzegorczyk, A., Malm, A., Skalicka-Woźniak, K., 2015. Bioactivity-guided isolation of antimicrobial coumarins from Heracleum mantegazzianum Sommier & Levier (Apiaceae) fruits by high-performance counter-current chromatography. Food Chem. 186, 133–138.
Wang, C., Cao, B., Liu, Q.Q., Zou, Z.Q., Liang, Z.A., Gu, L., Dong, J.P., Liang, L.R., Li, X.W., Hu, K., He, X.S., Sun, Y.H., An, Y., Yang, T., Cao, Z.X., Guo, Y.M., Wen, X.M., Wang, Y.G., Liu, Y.L., Jiang, L.D., 2011. Oseltamivir compared with the Chinese traditional therapy maxingshigan-yinqiaosan in the treatment of H1N1 influenza: a randomized trial. Ann. Intern. Med. 155 (4), 217–246.
Wang, W., Zhang, P., Hao, C., Zhang, X.-E., Cui, Z.-Q., Guan, H.-S., 2011a. In vitro inhibitory effect of carrageenan oligosaccharide on influenza A H1N1 virus. Antivir. Res. 92 (2), 237–246.
Watanabe, K., Ishikawa, T., Otaki, H., Mizuta, S., Hamada, T., Nakagaki, T., Ishibashi, D., Urata, S., Yasuda, J., Tanaka, Y., Nishida, N., 2017. Structure-based drug discovery for combating influenza virus by targeting the PA-PB1 interaction. Sci. Rep. 7 (1), 9500.
Wei, W., Wan, H., Peng, X., Zhou, H., Lu, Y., He, Y., 2018. Antiviral effects of Ma Huang Tang against H1N1 influenza virus infection in vitro and in an ICR pneumonia mouse model. Biomed. Pharmacother. 102, 1161–1175.
Wurzer, W.J., Planz, O., Ehrhardt, C., Giner, M., Silberzahn, T., Pleschka, S., Ludwig, S., 2003. Caspase 3 activation is essential for efficient influenza virus propagation. EMBO J. 22 (11), 2717–2728.
Xian, Z., Jin, G., Li, H., Jiang, J., Wang, C., Zhu, L., Jin, Z., Li, L., Piao, H., Zheng, M., Yan, G., 2019. Imperatorin suppresses anaphylactic reaction and IgE-mediated allergic responses by inhibiting multiple steps of FceRI signaling in mast cells: IMP alleviates allergic responses in PCA. BioMed Res. Int. 2019, 7823761.
Yaeghoobi, M., Frimayanti, N., Chee, C.F., Ikram, K.K., Najjar, B.O., Zain, S.M., Abdullah, Z., Wahab, H.A., Rahman, N.A., 2016. QSAR, in silico docking and in vitro evaluation of chalcone derivatives as potential inhibitors for H1N1 virus neuraminidase. Med. Chem. Res. 25, 2133–2142.
Yeganeh, B., Ghavami, S., Rahim, M.N., Klonisch, T., Halayko, A.J., Coombs, K.M., 2018. Autophagy activation is required for influenza A virus-induced apoptosis and replication. Biochim. Biophys. Acta Mol. Cell Res. 1865 (2), 364–378.
Yeh, J.-Y., Coumar, M.S., Horng, J.-T., Shiao, H.-Y., Kuo, F.-M., Lee, H.-L., Chen, I.-C., Chang, C.-W., Tang, W.-F., Tseng, S.-N., Chen, C.-J., Shih, S.-R., Hsu, J.T., Liao, C.-C., Chao, Y.-S., Hsieh, H.-P., 2010. Anti-influenza drug discovery: structure-activity relationship and mechanistic insight into novel angelicin derivatives. J. Med. Chem. 53 (4), 1519–1533.
Zhang, X.N., Ma, Z.J., Wang, Y., Sun, B., Guo, X., Pan, C.Q., Chen, L.M., 2017. Angelica dahurica ethanolic extract improves impaired wound healing by activating angiogenesis in diabetes. PloS One 12 (5), e0177862.
Zhang, Y., Cao, Y., Wang, Q., Zheng, L., Zhang, J., He, L., 2011. A potential calcium antagonist and its antihypertensive effects. Fitoterapia 82 (7), 988–996.